Controlled Release and Assembly of Drug Nanoparticles via pH-Responsive Polymeric Micelles: A Theoretical Study

ARTICLE *in* THE JOURNAL OF PHYSICAL CHEMISTRY B · APRIL 2012

Impact Factor: 3.3 · DOI: 10.1021/jp3007816 · Source: PubMed

4 AUTHORS:

Guangkui Xu
Xi'an Jiaotong University
22 PUBLICATIONS **171** CITATIONS
SEE PROFILE

Xi-Qiao Feng
Tsinghua University
330 PUBLICATIONS **5,504** CITATIONS
SEE PROFILE

Bo Li
University of Maryland, College Park
288 PUBLICATIONS **4,469** CITATIONS
SEE PROFILE

Huajian Gao
Brown University
553 PUBLICATIONS **22,856** CITATIONS
SEE PROFILE

THE JOURNAL OF PHYSICAL CHEMISTRY B

Article

pubs.acs.org/JPCB

Controlled Release and Assembly of Drug Nanoparticles via pH-Responsive Polymeric Micelles: A Theoretical Study

Guang-Kui Xu,[†] Xi-Qiao Feng,*[,†] Bo Li,[§] and Huajian Gao[‡]

[†]Institute of Biomechanics and Medical Engineering, AML, Department of Engineering Mechanics, Tsinghua University, Beijing 100084, China

[§]College of Pharmaceutical Sciences, Zhejiang University, Hangzhou 310058, China

[‡]School of Engineering, Brown University, Providence, Rhode Island 02912, United States

ABSTRACT: Tumor tissues often have a pH value lower than normal tissues, and this difference suggests a promising way of targeted cancer therapy by using pH-controlled drug delivery systems. On the basis of the mean-field theory, we present a theoretical methodology to predict the self-assembly and disassembly of pH-responsive polymers and nanoparticles in an ionic solution. It is found that vesicles, cylindrical, and spherical micelles can rapidly disassemble and release contained nanoparticles in a narrow pH range. The model is further used to study the controlled assembly of pH-sensitive drug with significantly improved encapsulation efficiency. This method is also applicable for the design of controlled delivery nanodevices for various biomedical applications.

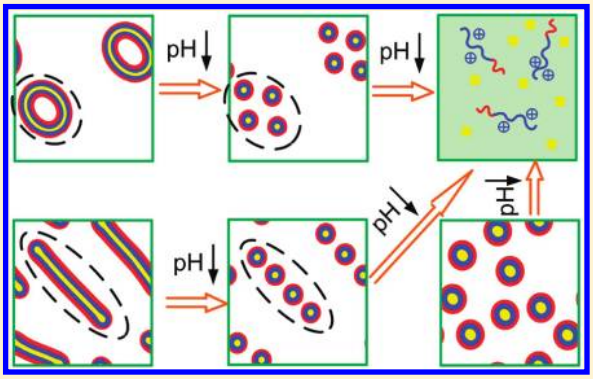

1. INTRODUCTION

The development of on-demand drug delivery techniques remains a challenging issue in the fields of nanobiotechnology, nanomedicine and pharmaceutics for disease diagnosis, cancer treatment, and gene therapy.[1−3] An ideal delivery device should be biocompatible, biodegradable, and can be easily triggered to release a certain dosage of drug molecules demanded by patients (e.g., local pain relief) or prescribed by doctors (e.g., localized chemotherapy).[4−6] Further, the enhanced therapeutic efficacy and minimal side effects require that the drug be released only at targeted locations. Controllable drug release in a specific tissue can be performed by incorporating release mechanisms triggered by environmental stimuli, e.g., pH,[7] temperature,[8] and light.[4]

Human body has distinct pH gradients in physiological and pathological states. For example, some solid tumor tissues form a mildly acidic environment (pH ∼ 6.5),[9,10] while blood and normal issues have a pH value of about 7.4. Cellular subcompartments such as endosomes (∼5.0−6.5) and lysosomes (∼4.5−5.0) have pH values distinctly lower than the cytosol.[11] Polymeric micelles represent a prominent class of drug delivery systems because they are biocompatible, capable of storing various drug molecules, and can be easily incorporated with pH-responsive elements.[3,12−15] Cullis and co-workers experimentally observed the transition between lamellar and inverted hexagonal structures of pH-sensitive vesicles with the variation of pH.[16−19] Recently, considerable experimental effort has been directed toward targeted delivery of cargos (e.g., drugs, proteins, and DNA and RNA molecules) by pH-responsive polymeric micelles.[7,20−22] These studies are calling for parallel development of theoretical methods to predict pH-controlled assembly and disassembly of pH-responsive polymer−drug micelles, which are of both technological and clinical interest.

In this paper, a theoretical approach is used to quantitatively model the controlled encapsulation and release of drug nanoparticles by pH-responsive polymeric micelles. This approach combines the self-consistent field theory (SCFT) for polymers, Poisson−Boltzmann equation for ionic interactions, and the density functional theory for the steric interaction between different particles (e.g., drug particles and large ions). This method can be used to predict pH-controlled assembly and release of molecules (e.g., drugs and proteins), as well as to design novel nanodevices for medical applications.

2. METHOD

Consider a system consisting of diblock copolymers and nanoparticles in an ionic solution. The diblock is formed by weak polyelectrolyte (WPE) blocks, whose charge density can be altered by changing environmental pH. Each diblock copolymer consists of N segments in total, including hydrophobic segments (A) and hydrophilic segments (B). The volume fraction of the A segments per chain is denoted as f. The nanoparticles (P) are used to model delivered cargos (e.g., drugs and globular proteins) and large ions in the solution. All small ions, coming from the dissociation of WPE blocks and dissolved salt, are treated as identical point charges denoted by "+" for cations and "−" for anions, respectively. Assume that

Received: January 24, 2012
Revised: April 27, 2012
Published: April 30, 2012

dx.doi.org/10.1021/jp3007816 | J. Phys. Chem. B 2012, 116, 6003−6009

the ions are all monovalent. The volume fractions of diblocks, nanoparticles and water are φ_D, φ_P and φ_W, respectively. All length parameters are normalized by the diblock radius of gyration, R_g.

Our method is based on the SCFT, which has proven to be a powerful tool to study complex morphologies of block copolymers and their blends.[23−27] The pair interactions between different species are determined by a set of chemical potential fields $W_I(\mathbf{r})$, defining the intensity of the mean field felt by species I at position $\mathbf{r}$. In the ionic solution, the electric interactions between charged species are taken into account. Li and Schick presented a microscopic theory to study the transition between the lamellar phase and the inverted hexagonal phase of pH-responsive vesicles by combining the SCFT for polymeric fluids and Poisson−Boltzmann equation for ionic interactions.[28,29] Since the SCFT method does not take into account the excluded volume interaction between particles,[30−34] we will consider this steric interaction by using the density functional theory. The dimensionless Helmholtz free energy of the system is[35−37]

$$F = F_{en} + F_{db} + F_{ml} + F_{np} + F_{el} \tag{1}$$

Here, F_{en} represents the enthalpic interactions between different components

$$F_{en} = \frac{1}{2V}\int d\mathbf{r} \sum_I \sum_{J\neq I} N\chi_{IJ}\phi_I(\mathbf{r})\phi_J(\mathbf{r}) \tag{2}$$

where V is the volume of the solution, χ_{IJ} is the Flory−Huggins interaction parameter between species I and J, and $\varphi_I(r)$ is the local volume fraction of species I. The entropic contribution of diblocks to the free energy, F_{db}, is expressed as

$$F_{db} = \varphi_D \ln\left(\frac{V\varphi_D}{Q_D}\right) - \frac{1}{V}\int d\mathbf{r} \sum_{I=A,B} [W_I(\mathbf{r})\phi_I(\mathbf{r}) + z_I\alpha_I(\mathbf{r})\psi(\mathbf{r})\phi_I(\mathbf{r})] \tag{3}$$

where Q_D is the partition function of a single chain, $\psi(\mathbf{r})$ is the electrostatic potential, α_I is the ionization degree of specie I, z_I = 1 for a polycation, and z_I = −1 for a polyanion. F_{ml} accounts for the entropic contributions from small molecules, including cations, anions, and water molecules, to the free energy:

$$F_{ml} = \sum_{m=+,-,W} N\varphi_m \ln\left(\frac{V\varphi_m}{Q_m}\right) - \frac{1}{V}\int d\mathbf{r}\,[W_W(\mathbf{r})\phi_W(\mathbf{r}) + \psi(\mathbf{r})\phi_+(\mathbf{r}) - \psi(\mathbf{r})\phi_-(\mathbf{r})] \tag{4}$$

where m designates cations (+), anions (−), or water molecules (W), and Q_m is the partition function of a single m molecule. On the basis of the mean field theory, the entropic contribution of nanoparticles to the free energy, F_{np0}, is[30−34]

$$F_{np0} = \sum_{PS} \frac{\varphi_{PS}}{\beta_{PS}} \ln\left(\frac{V\varphi_{PS}}{Q_{PS}\beta_{PS}}\right) - \frac{1}{V}\int d\mathbf{r}\, W_{PS}(\mathbf{r})\rho_{PS}(\mathbf{r}) \tag{5}$$

where PS designates the particle of type S, β_{PS} is the volume ratio of a particle of type S to a diblock chain, Q_{PS} is the partition function of a single particle of type S, and ρ_{PS} is the particle distribution function. The excluded volume interaction between particles is considered by the density functional theory, and the entropic contribution of nanoparticles can be expressed as[32−34]

$$F_{np} = F_{np0} + \frac{1}{V}\int d\mathbf{r}\, \rho_{PS}(\mathbf{r})\Psi(\bar{\phi}_{PS}, \{x_{PH}\}) \tag{6}$$

where $\bar{\phi}_{PS}$ is the "weighted" densities, x_{PH} is the number fraction, and Ψ is the excess free energy per particle accounting for the excluded volume interactions between particles. The number fraction x_{PS} is

$$x_{PS} = \frac{\varphi_{PS}}{\beta_{PS}\sum_{PL}\frac{\varphi_{PL}}{\beta_{PL}}} \tag{7}$$

The local volume fraction $\phi_{PS}(\mathbf{r})$ and the "weighted" nonlocal volume fraction $\bar{\phi}_{PS}(\mathbf{r})$ are given by

$$\phi_{PS}(\mathbf{r}) = \frac{\beta_{PS}}{v_S}\int_{|\mathbf{r}'|<R_S} d\mathbf{r}'\, \rho_{PS}(\mathbf{r}+\mathbf{r}') \tag{8}$$

$$\bar{\phi}_{PS}(\mathbf{r}) = \sum_{PL}\frac{\beta_{PL}}{v_{S+L}}\int_{|\mathbf{r}'|<R_S+R_L} d\mathbf{r}'\, \rho_{PL}(\mathbf{r}+\mathbf{r}') \tag{9}$$

where v_S and v_{S+L} represent the volumes of a sphere of radii R_S and $R_S + R_L$, respectively. For multiple species of particles, the exclude volume interactions between particles can be calculated by using the Boublik−Mansoori−Carnahan−Starling−Leland equation of state based on the density functional theory[38,39]

$$\Psi(\phi, \{x_i\}) = -\frac{4\phi - 3\phi^2}{(1-\phi)^2} - \frac{3}{2}\left[\frac{1}{(1-\phi)^2} - 1\right]\sum_{j>i=1}^{u}\frac{x_i x_j (R_i + R_j)(R_i - R_j)^2}{\eta} - \frac{3\phi^2}{2(1-\phi)^2}\sum_{j>i=1}^{u}\frac{x_i x_j R_i R_j (R_i - R_j)^2}{\eta^2} - \sum_{k=1}^{u} x_k R_k{}^2 - \left[\frac{2\phi - 3\phi^2}{2(1-\phi)^2} + \ln(1-\phi)\right]\left[1 - \frac{1}{\eta^2}\left(\sum_{k=1}^{u} x_k R_k{}^2\right)^3\right] \tag{10}$$

where u is the number of species of particles, ϕ is the total volume fraction of particles, x_i is the number fraction of particles of type i, R_i is the radius of particles of type i, and $\eta = \sum_{i=1}^{u} x_i R_i^3$. If there is only one type of particles, the BMCSL equation reduces to the Carnahan−Starling formula[40]

$$\Psi(\phi) = -\frac{4\phi - 3\phi^2}{(1-\phi)^2} \tag{11}$$

In eq 1, F_{el} denotes the energy resulting from electrostatic interactions in the ionic solution:[36,41]

$$F_{el} = \frac{1}{V}\int d\mathbf{r}\left[\phi_e(\mathbf{r})\psi(\mathbf{r}) - \frac{1}{2}\varepsilon|\nabla\psi(\mathbf{r})|^2\right] \tag{12}$$

where ε is the dielectric constant of the medium and $\phi_e(\mathbf{r})$ is the charge density. The electrostatic potential $\psi(\mathbf{r})$ can be obtained through the Poisson−Boltzmann equation

$$\varepsilon\nabla^2\psi(\mathbf{r}) = -\phi_e(\mathbf{r}) \tag{13}$$

where

dx.doi.org/10.1021/jp3007816 | J. Phys. Chem. B 2012, 116, 6003−6009

$$\phi_e(\mathbf{r}) = \phi_+(\mathbf{r}) - \phi_-(\mathbf{r}) + \sum_{I=A,B} z_I \alpha_I(\mathbf{r}) \phi_I(\mathbf{r}) \quad (14)$$

For weak polyelectrolytes, the ionization degree α_I, representing their dissociative probability, is given by[42,43]

$$\alpha_I(\mathbf{r}) = [1 + 10^{z_I(\mathrm{pH}-\mathrm{pK}_I)} e^{z_I \psi(\mathbf{r})}]^{-1} \quad (15)$$

where $\mathrm{p}K_I$ is the intrinsic pK value of species I. In the case of strong polyelectrolytes, the ionization degree α_I is the charged fraction of polyelectrolyte blocks[42,43]

$$\alpha_I(\mathbf{r}) = [1 + 10^{z_I(\mathrm{pH}-\mathrm{pK}_I)}]^{-1} \quad (16)$$

In this study, we only consider weak polyelectrolytes because of their wide application in drug delivery systems.

The variation of the free energy F with respect to φ_I, W_I, and ψ yields a system of equations, which, in conjunction with the incompressible condition $\sum_I \phi_I = 1$, form a closed set of equations. They are solved self-consistently in a two-dimensional 256 × 256 square lattice with periodic boundary conditions. The system is thought to have reached equilibrium when the relative difference between the free energies of the system at two neighboring iteration steps is less than 0.001%. In each case, we repeat the simulations for many times using different random numbers to ensure that the obtained structures are not accidental.

This method can account for the effects of incompatible interaction between different species, the conformational entropy of polymer chains, the excluded volume interaction between particles, and the electrostatic interaction. It is applicable to problems involving pH-controlled assembly and release of chain molecule (e.g., polyelectrolytes) as well as particles (e.g., drug particles and globular proteins).

3. RESULTS AND DISCUSSION

In recognition of the difference in pH values between tumoral (pH~6.5) and normal issues (pH~7.4),[9,10] here we consider an acid-responsive diblock copolymer that can self-assemble into micelles in an alkaline environment and disassemble into monomers when that environment turns into acidic. To compare with relevant experiments of pH-responsive PMPC-*b*-PDPA vesicles,[22] we regard PDPA and PMPC blocks as A- and B-blocks, respectively. The PDPA chain contains polybase blocks with $\mathrm{p}K_a$ = 6.3,[22] which can be progressively protonated with decreasing pH. Since the A-blocks and B-blocks are hydrophobic and hydrophilic, respectively, their interaction parameter is taken to be χ_{AB} = 0.9. Because water molecules have a preferential interaction to the B-blocks, their interaction parameter is set as χ_{BW} = −0.1. The drug particles are set to be hydrophobic since most anticancer drugs are hydrophobic. Then, the interaction parameter between drug particles and hydrophobic A-blocks is assumed to be χ_{AP} = 0. Other interactions between different species are taken as $\chi_{AW} = \chi_{PW} = \chi_{BP}$ = 1.0. The salt concentration is fixed at 0.1 M, as in the physiological condition. The volume fractions of drug particles and large ions are set as φ_{PD} = 0.04 and φ_{PI} = 0.03, and their radii are $R_{PD} = 0.75R_g$ and $R_{PI} = 0.5R_g$, respectively. For the other parameters, we set N = 50, ε = 1, and ϕ_A = 0.069. According to relevant studies,[25,27] the values of these parameters have been taken in a reasonable range. Our simulations demonstrate that these parameters do not qualitatively interfere with the results of the self-assembly of block copolymers and the dissociation of vesicles or micelles with which we concern ourselves in this paper.

3.1. Validation of the Method. To validate the proposed method, we first examine the morphological transitions of acid-sensitive copolymers with decreasing pH under three representative cases (Figure 1) and compare the theoretical results with relevant experimental observations in the literature.

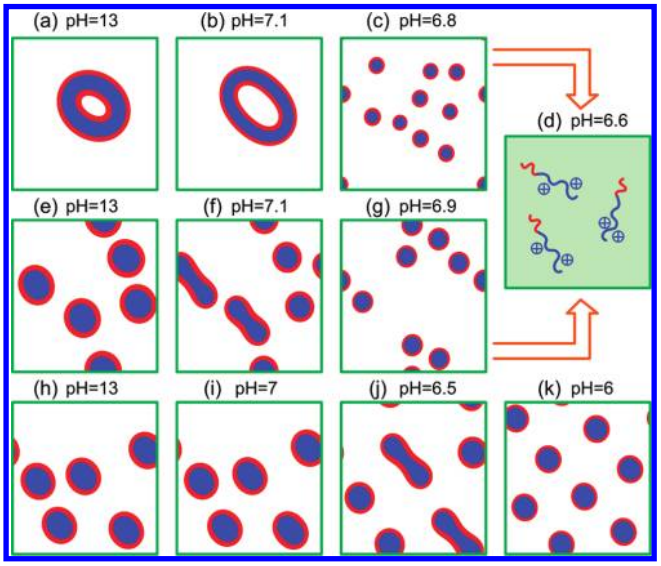

Figure 1. pH-induced morphological transitions of acid-sensitive diblock copolymer micelles: (a–d) morphological transitions of a vesicle (f = 0.92) with hydrophobic polybase blocks, (e–g, d) morphological transitions of spherical micelles (f = 0.84) with hydrophobic polybase blocks, and (h–k) morphological transitions of spherical micelles (f = 0.84) with hydrophilic polybase blocks. The blue, red, and white colors represent high concentration regions of A-blocks, B-blocks, and water molecules, respectively.

In the first case, a copolymer with hydrophobic polybase blocks (f = 0.92) is seen to self-assemble into a vesicle at pH = 13 (Figure 1a). Equation 15 shows that the ionization degree will become negligibly small when the environmental pH is significantly higher than the intrinsic pK value of the polybase blocks, $\mathrm{p}K_a$ = 6.3. As pH decreases, the ionization degree will increase, and the hydrophobic polybase (A) blocks will be progressively protonated and positively charged. When pH reduces to 7.1, the charged A-blocks repel each other, resulting in vesicle swelling (Figure 1b). A sharp morphological transition occurs at pH = 6.8, at which the vesicle disassembles into many small spherical micelles (Figure 1c). This disassembly is attributed to the rapid increase in the protonated fraction of A-blocks when pH approaches their intrinsic pK value, $\mathrm{p}K_a$. The strong electrostatic repulsion between A-blocks destroys the vesicle and breaks it into many small spherical micelles. At this point, a slight decrease in pH (6.6) will induce the spherical micelles to further dissociate into monomers (Figure 1d). This theoretical result agrees with the experimental observations of Du et al.[22] and Borchert et al.[44] that the polymeric vesicles can disassemble into monomers in a narrow pH range.

The second case involves a copolymer with hydrophobic polybase (A) blocks (f = 0.84) self-assembling into spherical micelles at pH = 13 (Figure 1e). As pH decreases, the hydrophobic cores are progressively protonated, resulting in the formation of cylindrical micelles (pH = 7.1; Figure 1f). At pH =

dx.doi.org/10.1021/jp3007816 | J. Phys. Chem. B 2012, 116, 6003–6009

6.9, the enhanced electrostatic repulsion between charged A-blocks facilitates the degradation of cylindrical micelles into more spherical micelles (Figure 1g). A further decrease in pH will induce rupture and complete disassembly of the micelles (Figure 1d). This theoretical prediction agrees with recent experiments[45−48] that the spherical micelles will disassemble into monomers within a sharp range of pH, due to the rapid protonation of block copolymers when the pH value is close to the value of pK_a.

In the third case, a copolymer with hydrophilic polybase (B) blocks (f = 0.84) self-assembles into spherical micelles at pH = 13 (Figure 1h). With decreasing pH, B-blocks are progressively protonated. The strong electrostatic repulsion between hydrophilic shells formed by B-blocks will elongate the spherical micelles to a cylindrical shape at pH = 6.5, as shown in Figure 1j. When pH reduces to 6.0, the strongly charged hydrophilic B-blocks will facilitate the degradation of the cylindrical micelles into smaller spherical micelles (Figure 1k). A further decrease in pH will not change the morphology further (results not shown). This pH-induced phase transition between large spherical micelles and small spherical micelles concurs with Xu et al's experimental results.[49] In their experiments, large spherical micelles evolve into small spherical micelles as pH decreases to a critical value, due to the same physical mechanisms at play in our simulations.

The morphological transitions of acid-responsive block copolymers in the above three cases all agree with relevant experiments, demonstrating the efficacy of the present method. Moreover, our findings show that when the hydrophobic (A) blocks are pH-responsive, the micelles can sharply disassemble into monomers within a narrow pH range. In what follows, we will only consider pH-sensitive hydrophobic blocks, since their capability of pH-controlled disassembly permits the control of drug release.

3.2. pH-Controlled Drug Release. In this subsection, we study the morphological transitions of pH-sensitive copolymers and the associated release of nanoparticles with respect to pH (Figure 2). Under different copolymer compositions f, the blend can self-assemble into various morphologies in an alkaline solution (pH 13). For f = 0.84, the blend self-assembles into a spherical micelle containing hydrophobic drugs in its core (Figure 2h). With increasing f, the longer hydrophobic chains tend to elongate the spherical micelles into cylindrical micelles (f = 0.9; Figure 2d) and, subsequently, into vesicles (f = 0.92; Figure 2a). This morphological transition induced by the copolymer composition is consistent with relevant experimental observations.[50,51]

Next, we examine the disassembly of micelles of different shapes and the associated drug release as the environmental pH varies. Figure 2, parts a−c and part g show the vesicle disassembly with decreasing pH. As the pH reduces to 6.9, the vesicle swells due to enhanced repulsion between the progressively charged A-blocks (Figure 2b). At pH = 6.7, each vesicle disassembles into many small spherical micelles (Figure 2c) because the largely protonated A-blocks repel each other. Further decrease of pH to 6.5 will induce the micelles to dissociate into monomers, rendering a quick and complete release of drug particles (Figure 2g). This result is in agreement with the experimental phenomenon that an acid-responsive vesicle containing hydrophobic particles dissociates into monomers as pH falls below a critical value.[22]

Figure 2d−g show the disassembling process of cylindrical micelles as pH varies from an alkaline to a mildly acidic

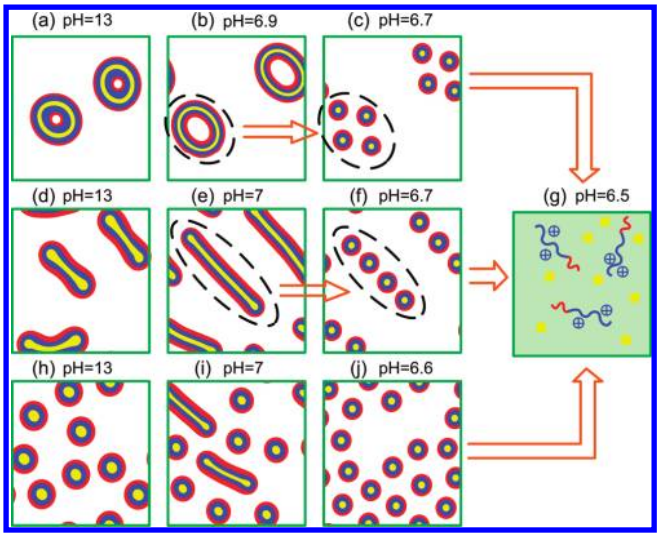

Figure 2. pH-induced disassembly of acid-responsive diblock copolymer micelles loaded with drug particles. Snapshot configurations show the morphological disassembly of (a−c, g) vesicles, (d−g) cylindrical micelles, and (h−j, g) spherical micelles as pH decreases. The blue, red, yellow, and white colors represent high concentration regions of A-blocks, B-blocks, drug particles, and water molecules, respectively.

environment. As shown in Figure 2e, the cylindrical micelles are stretched to longer and thinner cylinders when pH reduces to 7.0. This is due to the stronger electrostatic repulsion between progressively charged A-blocks with decreasing pH. At pH = 6.7, the enhanced electrostatic repulsion facilitates the fragmentation of long cylindrical micelles into many smaller spherical micelles (Figure 2f). After that, a further drop in pH will cause complete disassembly of spherical micelles (Figure 2g), indicating all drugs are released. Figure 2h−j and 2g show the disassembling process of spherical micelles with respect to pH. The apparent behavior is quite similar to that for cylindrical micelles except that some spheres are elongated into cylinders at pH = 7.0 (Figure 2i).

To quantitatively illustrate the effect of pH on drug release, we plot the drug content in micelles as a function of pH in Figure 3, showing a pH-induced drug release profile. Each point in Figure 3 corresponds to a simulation result. At the initial state (pH = 13), the vesicles have a higher drug content than cylindrical and spherical micelles. All drug molecules in the

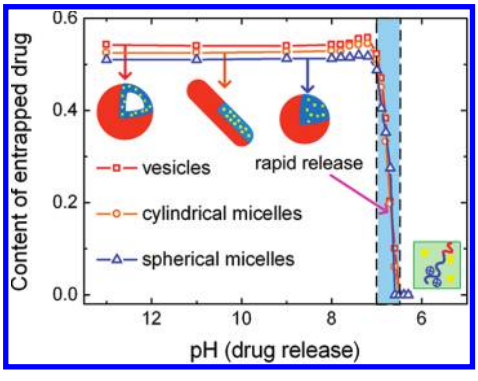

Figure 3. Entrapped drug content in vesicles (red), cylindrical (orange) and spherical (blue) micelles as a function of pH, indicating the pH-induced drug release profiles. Each point in the figure corresponds to a simulation result.

dx.doi.org/10.1021/jp3007816 | J. Phys. Chem. B 2012, 116, 6003−6009

three types of micelles are rapidly released in a narrow pH range of 7.0−6.5, in consistency with the results in Figure 2. This demonstrates that a slight variation of pH can induce quick disassembly of pH-responsive polymer-drug micelles, indicating the potential of such systems for targeted delivery to tumor tissues with special pH environments.

3.3. Design Strategy to Improve the Encapsulation Efficiency of Drug. The efficiency of drug encapsulation is another major concern in the development of nanomedicine for cancer therapy. Figure 3 shows that the encapsulation efficiencies of drug in the three representative types of micelles are all lower than 60%. In what follows, we propose a pH-controlled assembly method to improve the loading capacity of micelles based on our theoretical prediction. Since the polybase blocks are cationic when protonated, more drug molecules can be encapsulated in micelles if they are anionic. However, anionic drug molecules could be difficult to be released due to their strong attraction with cationic polybase blocks. Therefore, an ideal drug should be anionic when they are encapsulated, and be stripped off charges when they need to be released. In other words, the drug should be base-sensitive, and such a property can be achieved by grafting weakly acidic groups on the drug molecules.

To test the drug design strategy suggested above, we simulate the self-assembled morphologies of the blend under different pH conditions (Figure 4) and calculate the corresponding

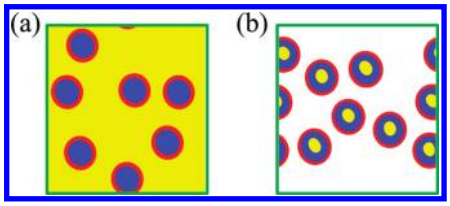

Figure 4. Self-assembled morphologies of acid-sensitive copolymers with pK_a = 6.3 and base-sensitive drugs with pK_d = 8.5 under different pH values: (a) pH = 8.4; (b) pH = 7.2. The blue, red, yellow and white colors represent high concentration regions of A-blocks, B-blocks, drug and water molecules, respectively. Water molecules are not shown in part a.

encapsulation efficiencies (Figure 5). Let pK_d denote the intrinsic pK value of drug particles. Figure 4 shows the morphologies of the acid-sensitive copolymer and the base-sensitive drug under two representative pH values, for the

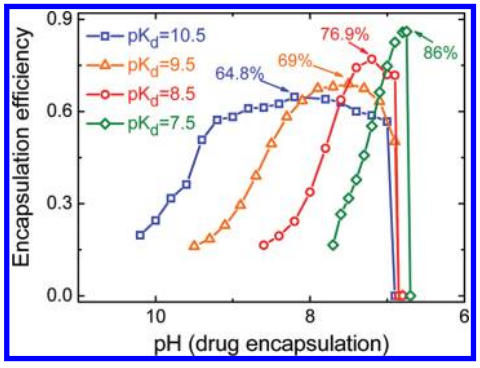

Figure 5. Encapsulation efficiency of base-sensitive drugs under four pK_d values as a function of pH. The highest encapsulation efficiency of each case is pointed out in the figure. Each point in the figure corresponds to a simulation result.

spherical micelle-forming composition of f = 0.84 and pK_d = 8.5. When the pH is near the pK_d (e.g., pH = 8.4), the ionization degree of drugs is large and the charged drug molecules repel each other, resulting in the dissolution of drugs, whereas the copolymers are almost uncharged and form spherical micelles (Figure 4a). As pH reduces to 7.2, some drugs are negatively charged and a certain part of copolymers are positively charged. The stronger electrostatic attraction facilitates a larger fraction of drugs to be encapsulated into the core of spherical micelles, as show in Figure 4b. Although there is still a lack of direct experimental evidence to verify our theoretical prediction, Giacomelli et al. experimentally observed that base-sensitive particles can be highly encapsulated in acid-sensitive polymeric micelles, implying that the above design strategy is a promising route to improving the encapsulation efficiency of drug.[48]

Corresponding to Figure 4, the encapsulation efficiencies of drug under four pK_d values are plotted as a function of pH, as shown in Figure 5. Each point corresponds to a simulation result. It can be seen that there is an optimal pH value to achieve the highest encapsulation efficiency in each case, which is significantly higher than that of the untreated drug (51.7%; Figure 3). When pH approaches pK_d, the micelle can only entrap a small amount of drug because most drug particles are ionized in the solution, as shown in Figure 4a. In comparison, when pH approaches pK_a, much of the copolymer is ionized and dissolved in the solution and no micelle can be formed. Thus, only when pH takes a critical value between pK_a and pK_d, can the fraction between charged drugs and charged polymers reach an optimal balance, at which a maximum amount of negatively charged drugs will be entrapped in positively charged micelles.

Finally, we examine whether this polymeric micelle with base-sensitive drug can still disassemble in the designed range of pH. As pH decreases from the optimal pH value in Figure 5, the drug content in micelles is plotted in Figure 6, where each

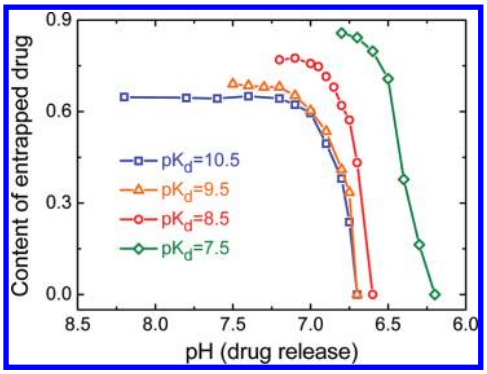

Figure 6. Content of encapsulated drug in micelles as pH decreases from the optimal pH values in Figure 5, showing the pH-induced drug release profiles. Each point in the figure corresponds to a simulation result.

point corresponds to a simulation result. The profiles reveal that the micelles can quickly release the contained drug in a narrow pH range. Therefore, this pH-controlled assembly method can significantly improve the loading capacity without diminishing the controlled release efficiency of pH-responsive micelles. Further, it is interesting to note that the pH value (6.2) for complete drug release in the case of pK_d = 7.5 is lower than those (~6.7) in the other cases. If pK_d is closer to pK_a,

dx.doi.org/10.1021/jp3007816 | J. Phys. Chem. B 2012, 116, 6003−6009

there are more charged drug and copolymer at the optimal encapsulation pH. Since the attraction between anionic drug and cationic copolymer is strong, the experimental pH should take a lower value to release the drug. At a lower pH value, there will be less anionic drug and more cationic copolymer in the solution, meaning that the attraction between the drug and the copolymer will become weaker and the electrostatic repulsion between anionic copolymers will become stronger. Li and Schick pointed out that the difference between the intrinsic pK value of lipid headgroups and the solution pH is important for the structure of lipid vesicles.[29] As an additional aspect, our simulations show that the difference between the intrinsic pK values of pH-sensitive polymers and pH-sensitive drug particles plays a key role in the encapsulation and release of drug. This pH control method of drug release may be used to produce delivery devices that can release drug at a specified pH environment.

4. CONCLUSIONS

In summary, a theoretical method has been applied to predict pH-controlled assembly and disassembly of pH-responsive polymeric micelles for drug encapsulation, delivery and release. Using this method, it has been demonstrated that micelles of different shapes (vesicles, cylindrical and spherical micelles) can disassemble and completely release their cargos within a designable narrow range of pH. We also suggest a pH-controlled assembly method to improve the loading capacity of micelles. The difference between the intrinsic pK values of pH-sensitive polymers and drug particles is a key parameter to control the assembly and release of drug nanoparticles. It might be possible to apply this method to design controlled drug delivery devices that target tumor tissues and to study pH-triggered intracellular release of protein molecules in the field of gene therapy.

AUTHOR INFORMATION

Corresponding Author

*Telephone: +86-10-6277 2934. Fax: +86-10-6278 1824. E-mail: fengxq@tsinghua.edu.cn.

Notes

The authors declare no competing financial interest.

ACKNOWLEDGMENTS

Supports from the National Natural Science Foundation of China (Grants Nos. 10972121 and 107320503), the Ministry of Education (SRFDP 20090002110047), and the 973 program of MOST (2010CB631005 and 2012CB934101) are acknowledged.

REFERENCES

(1) Ferrari, M. *Nat. Rev. Cancer* **2005**, *5*, 161−171.
(2) Peer, D.; Karp, J. M.; Hong, S.; Farokhzad, O. C.; Margalit, R.; Langer, R. *Nature Nanotechnol.* **2007**, *2*, 751−760.
(3) Torchilin, V. P. *Nat. Rev. Drug Discov.* **2005**, *4*, 145−160.
(4) Febvay, S.; Marini, D. M.; Belcher, A. M.; Clapham, D. E. *Nano Lett.* **2010**, *10*, 2211−2219.
(5) Epstein-Barash, H.; Orbey, G.; Polat, B. E.; Ewoldt, R. H.; Feshitan, J.; Langer, R.; Borden, M. A.; Kohane, D. S. *Biomaterials* **2010**, *31*, 5208−5217.
(6) Hoare, T.; Santamaria, J.; Goya, G. F.; Irusta, S.; Lin, D.; Lau, S.; Padera, R.; Langer, R.; Kohane, D. S. *Nano Lett.* **2009**, *9*, 3651−3657.
(7) Hu, Y.; Litwin, T.; Nagaraja, A. R.; Kwong, B.; Katz, J.; Watson, N.; Irvine, D. J. *Nano Lett.* **2007**, *7*, 3056−3064.
(8) Qin, S. H.; Geng, Y.; Discher, D. E.; Yang, S. *Adv. Mater.* **2006**, *18*, 2905−2909.
(9) Sawant, R. R.; Torchilin, V. P. *Soft Matter* **2010**, *6*, 4026−4044.
(10) Vaupel, P.; Kallinowski, F.; Okunieff, P. *Cancer Res.* **1989**, *49*, 6449−6465.
(11) Schmaljohann, D. *Adv. Drug Deliver. Rev.* **2006**, *58*, 1655−1670.
(12) Rijcken, C. J. F.; Soga, O.; Hennink, W. E.; van Nostrum, C. F. *J. Controlled Release* **2007**, *120*, 131−148.
(13) Klaikherd, A.; Nagamani, C.; Thayumanavan, S. *J. Am. Chem. Soc.* **2009**, *131*, 4830−4838.
(14) Schroeder, A.; Kost, J.; Barenholz, Y. *Chem. Phys. Lipids* **2009**, *162*, 1−16.
(15) Szebeni, J.; Muggia, F.; Gabizon, A.; Barenholz, Y. *Adv. Drug Deliver. Rev.* **2011**, *63*, 1020−1030.
(16) Hope, M. J.; Cullis, P. R. *Biochem. Biophys. Res. Commun.* **1980**, *92*, 846−852.
(17) Hope, M. J.; Walker, D. C.; Cullis, P. R. *Biochem. Biophys. Res. Commun.* **1983**, *110*, 15−22.
(18) Hafez, I. M.; Cullis, P. R. *Biochim. Biophys. Acta* **2000**, *1463*, 107−114.
(19) Hafez, I. M.; Ansell, S.; Cullis, P. R. *Biophys. J.* **2000**, *79*, 1438−1446.
(20) Ganta, S.; Devalapally, H.; Shahiwala, A.; Amiji, M. *J. Controlled Release* **2008**, *126*, 187−204.
(21) Lee, Y.; Fukushima, S.; Bae, Y.; Hiki, S.; Ishii, T.; Kataoka, K. *J. Am. Chem. Soc.* **2007**, *129*, 5362−5363.
(22) Du, J. Z.; Tang, Y. P.; Lewis, A. L.; Armes, S. P. *J. Am. Chem. Soc.* **2005**, *127*, 17982−17983.
(23) Fredrickson, G. H. *The Equilibrium Theory of Inhomogeneous Polymers*; Oxford University: Oxford, U.K., 2006.
(24) Matsen, M. W.; Schick, M. *Phys. Rev. Lett.* **1994**, *72*, 2660−2663.
(25) Xu, G. K.; Li, Y.; Li, B.; Feng, X. Q.; Gao, H. J. *Soft Matter* **2009**, *5*, 3977−3983.
(26) Xu, G. K.; Lu, W.; Feng, X. Q.; Yu, S. W. *Soft Matter* **2011**, *7*, 4828−4832.
(27) Xu, G. K.; Feng, X. Q.; Li, Y. *J. Phys. Chem. B* **2010**, *114*, 1257−1263.
(28) Li, X. J.; Schick, M. *Biophys. J.* **2000**, *78*, 34−46.
(29) Li, X. J.; Schick, M. *Biophys. J.* **2001**, *80*, 1703−1711.
(30) Thompson, R. B.; Ginzburg, V. V.; Matsen, M. W.; Balazs, A. C. *Science* **2001**, *292*, 2469−2472.
(31) Thompson, R. B.; Ginzburg, V. V.; Matsen, M. W.; Balazs, A. C. *Macromolecules* **2002**, *35*, 1060−1071.
(32) Thompson, R. B.; Lee, J. Y.; Jasnow, D.; Balazs, A. C. *Phys. Rev. E* **2002**, *66*, 031801.
(33) Lee, J. Y.; Thompson, R. B.; Jasnow, D.; Balazs, A. C. *Phys. Rev. Lett.* **2002**, *89*, 155503.
(34) Liang, Q.; Ma, Y. Q. *Eur. Phys. J. E* **2008**, *25*, 129−138.
(35) Wang, Q.; Taniguchi, T.; Fredrickson, G. H. *J. Phys. Chem. B* **2004**, *108*, 6733−6744.
(36) Shi, A. C.; Noolandi, J. *Macromol. Theor. Simul.* **1999**, *8*, 214−229.
(37) Kumar, R.; Muthukumar. *J. Chem. Phys.* **2009**, *131*, 194903.
(38) Boublik, T. *J. Chem. Phys.* **1970**, *53*, 471−472.
(39) Mansoori, G.; Carnahan, N.; Starling, K.; Leland, T., Jr *J. Chem. Phys.* **1971**, *54*, 1523−1525.
(40) Carnahan, N. F.; Starling, K. E. *J. Chem. Phys.* **1969**, *51*, 635−636.
(41) Man, X.; Yang, S.; Yan, D.; Shi, A.-C. *Macromolecules* **2008**, *41*, 5451−5456.
(42) Biesheuvel, P. M. *Eur. Phys. J. E* **2005**, *16*, 353−359.
(43) Borukhov, I.; Andelman, D.; Orland, H. *Eur. Phys. J. B* **1998**, *5*, 869−880.
(44) Borchert, U.; Lipprandt, U.; Bilang, M.; Kimpfler, A.; Rank, A.; Peschka-Süss, R.; Schubert, R.; Lindner, P.; Förster, S. *Langmuir* **2006**, *22*, 5843−5847.
(45) Kim, M. S.; Hwang, S. J.; Han, J. K.; Choi, E. K.; Park, H. J.; Kim, J. S.; Lee, D. S. *Macromol. Rapid Commun.* **2006**, *27*, 447−451.

(46) Martin, T. J.; Procházka, K.; Munk, P.; Webber, S. E. *Macromolecules* **1996**, *29*, 6071−6073.
(47) Giacomelli, C.; Men, L. L.; Borsali, R. *Biomacromolecules* **2006**, *7*, 817−828.
(48) Giacomelli, C.; Schmidt, V.; Borsali, R. *Langmuir* **2007**, *23*, 6947−6955.
(49) Xu, L.; Zhu, Z. C.; Borisov, O. V.; Zhulina, E. B.; Sukhishvili, S. A. *Phys. Rev. Lett.* **2009**, *103*, 118301.
(50) Zhang, L. F.; Eisenberg, A. *J. Am. Chem. Soc.* **1996**, *118*, 3168−3181.
(51) Jain, S.; Bates, F. S. *Science* **2003**, *300*, 460−464.